Proc. Natl. Acad. Sci. USA
Vol. 93, pp. 1601–1606, February 1996
Biochemistry

In vivo and *in vitro* characterization of the B1 and B2 zinc-binding domains from the acute promyelocytic leukemia protooncoprotein PML

(B-box domain/nuclear bodies)

KATHERINE L. B. BORDEN*, JOHN M. LALLY*, STEPHEN R. MARTIN†, NICOLA J. O'REILLY‡, ELLEN SOLOMON§, AND PAUL S. FREEMONT*¶

*Protein Structure Laboratory, ‡Peptide Synthesis Laboratory, and §Somatic Cell Genetics Laboratory, Imperial Cancer Research Fund, 44 Lincoln's Inn Fields, London, WC2A 3PX, United Kingdom; and †Division of Physical Biochemistry, National Institute for Medical Research, The Ridgeway, Mill Hill, London, NW7 1AA, United Kingdom

Communicated by Paul Nurse, Imperial Cancer Research Fund, London, U.K., November 22, 1995 (received for review August 31, 1995)

ABSTRACT **Acute promyelocytic leukemia (APL) has been ascribed to a chromosomal translocation event which results in a fusion protein comprising the PML protein and retinoic acid receptor α. PML is normally a component of a nuclear multiprotein complex which is disrupted in the APL disease state. Here, two newly defined cysteine/histidine-rich protein motifs called the B-box (B1 and B2) from PML have been characterized in terms of their effect on PML nuclear body formation, their dimerization, and their biophysical properties. We have shown that both peptides bind Zn^{2+}, which induces changes in the peptides' structures. We demonstrate that mutants in both B1 and B2 do not form PML nuclear bodies *in vivo* and have a phenotype that is different from that observed in the APL disease state. Interestingly, these mutations do not affect the ability of wild-type PML to dimerize with mutant proteins *in vitro*, suggesting that the B1 and B2 domains are involved in an additional interaction central to PML nuclear body formation. This report in conjunction with our previous work demonstrates that the PML RING-B1/B2 motif plays a fundamental role in formation of a large multiprotein complex, a function that may be common to those unrelated proteins which contain the motif.**

The human *PML* gene is associated with APL (acute promyelocytic leukemia), which arises due to a block in normal differentiation of promyelocytes (for review, see ref. 1). In APL cells, *PML* is fused with the retinoic acid receptor α (RARα) following a reciprocal chromosomal translocation t(15;17)(q22q21) (2–5). The PML protein has been shown to be part of a nuclear multiprotein complex distinct from small nuclear ribonucleoproteins and nucleoli (6–10). These PML nuclear bodies become disrupted in leukemic cells; however, treatment with retinoic acid reverses these changes (8–10). It has been shown that the PML–RARα fusion product can bind to both normal PML (8, 10) as well as RXR, another retinoic acid receptor family member (retinoid X receptor), forming heterodimers (11). This leads to speculation that there is a dominant-negative effect of PML–RARα over both the PML protein and the RXR pathways. PML, but not PML–RARα, has been shown to be a growth suppressor both *in vitro* and *in vivo* (12), suggesting that sequestration of normal PML by PML–RARα would affect the growth suppressor activity of PML and sequestration of RXR, the induction of differentiation (12). It is suggested that both events may be necessary for leukemogenesis (12, 13).

The *PML* coding sequence contains three novel cysteine-rich metal binding regions and a predicted α-helical coiled-coil (see refs. 2 and 14). The first region, the RING motif, defines a family of proteins expressed in organisms ranging from plants to viruses, several of which have been implicated in oncogenesis (for review, see ref. 15). Recently the three-dimensional structure of the PML RING finger has been determined and the structural information used to probe the importance of various structural features *in vivo* (16). Within the RING finger family, a second cysteine-rich motif has been identified called the B-box (14, 15, 17). Most B-box family members possess a RING finger and either one or two B-box motifs followed closely by a predicted α-helical coiled-coil dimerization domain forming a tripartite motif (5, 14). The spacing between the three elements of the motif is highly conserved among family members, suggesting that the positions of each domain relative to the others is of functional importance (5, 14).

The B-box family comprises a number of transcription factors, ribonucleoproteins, and protooncogene products, which includes PML, the ret finger protein (RFP) and TIF1(T18) (see ref. 15 and references therein). These proteins are oncogenic in humans and mice when found as translocations that include the tripartite domain recombined with other genes. Recently, TIF1 has been shown to interact with several nuclear receptors *in vivo* and is proposed to mediate the ligand-dependent transcriptional activation function of nuclear receptors (18). PML and TIF1 possess two B-box-like domains, which appear to form a subset of the B-box family as highlighted by the presence of an extra conserved cysteine residue (see Fig. 1). EFP, an estrogen-responsive gene product, is another family member that has two B-boxes and is thought to represent an estrogen-responsive transcription factor mediating phenotypic expression due to estrogen action (19). The B-box domain has been found in the breast cancer locus *1A1.3B* (20), which has one B-box and a coiled-coil domain and appears tightly linked to the *BRCA-1* gene, which interestingly possesses a RING finger but no B-box or coiled-coil domains (21, 22). B1 and B2 B-boxes are also present in a putative *ataxia-telangiectasia* group D protein (ATDC), which possesses the two B-box domains and a coiled-coil domain but no RING finger (23), suggesting that the B-box and RING fingers can have independent molecular functions.

The best characterized B-box domain thus far reported is that from *Xenopus* nuclear factor XNF7. Our previous work has shown that, although there are seven potential metal ligands, the XNF7 B-box peptide binds only one Zn^{2+} per molecule and the Zn^{2+} is bound tetrahedrally (24). Therefore, of the seven potential ligands conserved in XNF7 B-box (see Fig. 1), only four are used in Zn^{2+} ion ligation within the B-box monomer. We have now determined the ligation scheme and

The publication costs of this article were defrayed in part by page charge payment. This article must therefore be hereby marked "*advertisement*" in accordance with 18 U.S.C. §1734 solely to indicate this fact.

Abbreviations: APL, acute promyelocytic leukemia; RARα, retinoic acid receptor α; RXR, retinoid X receptor; RFP, ret finger protein.
*To whom reprint requests should be addressed.

three-dimensional structure of the XNF7 B-box domain in the presence of Zn^{2+} (25). The B-box structure comprises two β-strands, two helical turns, and three extended loop regions and represents a novel zinc finger fold with an unusual ligation scheme. The conserved residues used in ligation are labeled in Fig. 1. Interestingly, two of the three remaining conserved residues, Cys-17 and Cys-25 as well as Asp-20, which is a cysteine in PML B1 and B2, are on a flexible loop in the XNF7 B-box structure (Fig. 1B). Mutations of Cys-17, Cys-25, and Asp-20 did not affect the ability of the XNF7 B-box monomer to fold or bind Zn^{2+} (25). This suggests that these conserved residues might form a potential interface for association with other proteins via metal-mediated intermolecular interaction. In the human immunodeficiency virus (HIV) Tat protein, for example, conserved metal ligands are used to form intermolecular dimers using divalent cations (26).

A number of studies have recently been initiated aimed at determining the molecular function of the B-box domain. Deletions of the XNF7 B-box domain results in a loss of binding to mitotic chromosomes (27), while deletions and point mutations in the B-box of PwA33 results in loss of association with the lampbrush loops of chromosomes in the oocyte nucleus in *Pleurodeles* (28, 42). These data at least suggest that the B-box domain of XNF7 and PwA33 is important for the association of these proteins with subcellular structures during *Xenopus* and *Pleurodeles* development, although the specific molecular interactions are at present unknown.

To better understand the function of the PML B1 and B2 B-box domains and their role in APL, we have analyzed both *in vivo* and *in vitro* site-directed mutations of conserved metal ligands within each domain. We have also carried out biophysical characterization of each domain. We show that both B1 and B2 bind Zn^{2+} and have apparent differences in their secondary structures. We also show that mutations of the B1 and B2 domains which in the XNF7 B-box homologue are not involved in monomer folding still cause disruption of PML nuclear bodies *in vivo*, without affecting PML homodimerization *in vitro*.

MATERIALS AND METHODS

Peptide Synthesis and Purification. The PML B1 (residues 124–166) and B2 (residues 184–232) peptides were synthesized on a model 431A Applied Biosystems solid-phase synthesizer and purified as described (24). Purified peptides (peak fractions from HPLC separations) were analyzed by matrix-assisted laser desorption mass spectrometry (29). Single species of B1 and B2 were observed with experimental molecular weights within 1 Da of the calculated masses for fully reduced forms of the peptides. The concentrations of B1 and B2 were measured optically using calculated extinction coefficients of 2.33 and 0.25 for a 1 mg/ml solution measured at 280 nm.

Optical Binding Studies of Cobalt. Typically, solutions (1 ml) containing 20–60 μM B1 and B2 peptide (10 mM Tris, pH 7.5) were titrated with solutions of $CoCl_2$ in the same buffer. The reaction was monitored on an HP 8452 diode array spectrometer using a 1-cm pathlength at room temperature. The spectra were corrected by subtracting the contribution from the peptide and buffer alone and normalized to an absorbance of zero at $\lambda = 800$ nm.

CD of the B1 and B2 B-Box Peptides. Samples for CD spectroscopy were prepared by dilution of stock peptide solution into a buffer containing 20 mM Pipes (pH 7.6) plus either 0.05 mM EDTA or the required metal ion (as the chloride), generally at a concentration of 0.2 mM. Far UV CD spectra were recorded from 260 to 195 nm using a Jasco J-600 spectropolarimeter operated with a time constant of 0.5 s. The spectra were recorded at 22°C for peptide solutions of ~0.05 or 0.02 mg/ml in 2- or 5-mm fused silica curvettes, respectively,

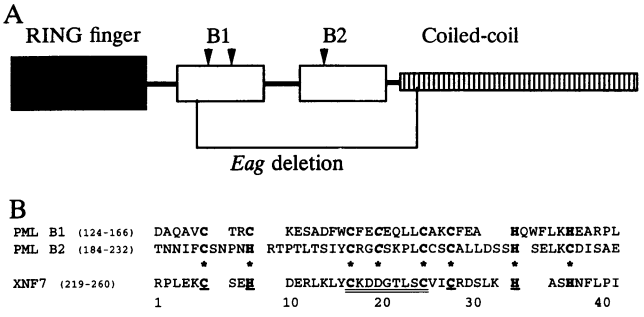

FIG. 1. (*A*) Tripartite domain for PML. B1 and B2 refer to B-boxes and coiled-coil refers to the predicted α-helical coiled-coil domain. Boundaries of the *Eag* deletion are also shown as well as the position of the double point mutations (▼). (*B*) Sequence alignment of PML B1 and B2 B-boxes and the XNF7 B-box for which the three-dimensional structure is known. Conserved cysteine and histidine residues are labeled (*) and are shown in boldface with those residues known to be Zn^{2+} ligands from the XNF7 B-box monomer structure (underlined). Extra conserved cysteine in PML B1 and B2 is in italics and is equivalent to Asp-20 in XNF7 B-box. Flexible loop region in XNF7 B-box (residues 17–25) is double underlined. Numbering refers to the XNF7 B-box peptide numbering and bracketed numbers refer to the whole protein sequence. Cys-21 and Cys-24 from PML B2 are equivalent to Cys-17 and Cys-20, respectively, in PML B1 and to Cys-20 and Asp-20 in XNF7 B-box.

and were the average of not less than four scans. All data reported here are presented as molar CD, $\Delta\varepsilon$ ($M^{-1}\cdot cm^{-1}$) based on a mean residue weight of 112.7. Residue molar ellipticity $[\theta]$ ($deg\cdot cm^2\cdot dmol^{-1}$) may be obtained from the relationship $[\theta]_{mrw} = 3300\Delta\varepsilon$.

Plasmids and Site-Directed Mutagenesis. Point mutations and a deletion were made in the 69-kDa isoform of PML. Mutagenesis was performed on the PML B1 and B2 B-boxes using a PCR stitching strategy (30) producing an *Eag* I fragment (420–800 bp). This *Eag* I fragment along with the remainder of the PML cDNA was cloned into a mammalian expression vector carrying the MLV enhancer (31). In total, three double point mutations were made as well as the *Eag* deletion. Constructs were sequenced to confirm the mutations. The modified PML genes were subcloned into the *Nco* I site in pLINK for *in vitro* translation experiments and into pAS for yeast two-hybrid experiments (yeast two-hybrid vectors were a gift of S. Elledge, Baylor College of Medicine, Houston).

PML Antibody, Transfection, and Immunofluorescence. PML (15–1745 bp) was bacterially expressed (pET-15b expression system; Novagen) and polyclonal antisera were raised as described (16). NIH 3T3 cells were transiently transfected using the DEAE-dextran shock method with ~8 μg of each construct (32) and after 40 h were fixed at −20°C in MeOH for 10 min prior to immunofluorescence studies. Transfected PML protein was detected using anti-PML polyclonal antiserum at a dilution of 1:200 followed by an anti-rabbit fluorescein isothiocyanate-conjugated secondary antibody at 1:200 dilution (Dakopatts, Glostrup, Denmark). Slides were analyzed by confocal microscopy with a 600 Bio-Rad instrument.

***In Vitro* Translation Studies.** Cotranslation experiments with the mutations in pLINK and 90-kDa PML isoform (wild type) with a C-terminal 9E10 tag also in pLINK were carried out using reticulocyte lysates (Promega) in the presence of [^{35}S]methionine and [^{35}S]cysteine similar to that described by Sambrook *et al.* (33). Translates were coimmunoprecipitated with the 9E10 monoclonal antibody and bovine serum albumin (0.5 mg/ml) and buffer E (50 mM Tris·HCl/150 mM NaCl/1 mM EDTA, pH 7.5). The 9E10 antibody was added to the lysates and left on ice for 20 min. Then protein A-Sepharose (Pharmacia) and anti-mouse antibody (Calbiochem) (1:1000 final dilution) were added and the samples were left to tumble

at 4°C for 1.5 h. Samples were washed twice in buffer E and 1% (vol/vol) Noridet P-40. The precipitates were boiled in reducing buffer and then subjected to SDS/15% PAGE and analyzed by autoradiography.

Yeast Two-Hybrid Assays. The PML-Eag deletion construct was subcloned into the pAS vector. The 69-kDa PML with a RING deletion in the pACT vector was a gift of N. Boddy (Imperial Cancer Research Fund, London). Yeast were grown in yeast extract/peptone/dextrose. The yeast SFY 526 strain was transfected using the lithium acetate protocol (34). Vectors were tested to show that they did not transactivate on their own. Transformed yeast were plated onto plates lacking tryptophan and leucine and incubated at 30°C for 2–3 days. Once the yeast was grown, colonies were lifted onto H-bond paper and permeabilized in liquid nitrogen and then placed on Whatman filter paper that had been soaked in Z-buffer (60 mM Na_2HPO_4/40 mM NaH_2PO_4/10 mM $MgCl_2$/50 mM 2-mercaptomethanol) containing 5-bromo-4-chloro-3-indolyl β-D-galactoside (1 mg/ml) at 30°C. Positive colonies appeared in 5 min to several hours (33).

RESULTS AND DISCUSSION

Optical Cobalt Binding Studies. The optical spectral properties of cobalt bound to synthetic Zn^{2+} finger peptides and purified proteins have been studied extensively and provide information on both the nature of the amino acid ligand and the geometry of ligation (26, 35–37). A series of titrations of the PML B-box domains B1 and B2, were carried out with solutions of cobalt (Fig. 2*A* and *B*, respectively). The resultant spectra showed absorption maxima at λ = 640–660 nm and shoulders at λ = 320 nm and 360–380 nm (Fig. 2). The 640- to 660-nm maxima are due to d-d transitions of Co(II) in a tetrahedral coordination and the charge transfer bands at 300–380 nm are a result of S-Co(II) coordination (35). This is consistent with previous results observed for the XNF7 B-box peptide (24). During the course of the cobalt titration, we observed no change for the overall spectrum except at high concentrations of cobalt when the peptide precipitated, causing scattering. Again, this is similar to the XNF7 B-box case where the peptide precipitated at high levels of cobalt. Due to misfolding, aggregation, and/or precipitation, not all of the peptides may be available for metal binding, resulting in an overestimation of the amount of competent peptide. Therefore, accurate values of binding constants and stoichiometry cannot be calculated. However, these results clearly show that cobalt binds to both PML B1 and B2 in a tetrahedral geometry using some cysteines as ligands.

Biophysical Characterization of B1 and B2 Synthetic Peptides. Structure formation upon metal ligation was monitored by CD. Fig. 3 shows the far UV CD spectrum of the B1 and B2 peptides in aqueous solution and in the same buffer after addition of Zn^{2+}. This region of the CD spectrum monitors the secondary structure content of the peptide. Interestingly, the spectrum of B1 (Fig. 3*A*) shows the presence of significant amounts of regular secondary structure (20–30% α-helix and some β-sheet) in the absence of added metal ion. This may be contrasted with the spectra of B2 (Fig. 3*B*) and XNF7 (24), which show little evidence for the presence of α-helix in the absence of added metal ion. The addition of metal ions to B1 produces a reduction in intensity, consistent with a loss of some α-helix and β-sheet. The addition of EDTA reverses the Zn^{2+}-induced change. Of a variety of metals tried, Ca^{2+}, Mg^{2+}, and Mn^{2+} induce no change; Cu^{2+} induces less change than Zn^{2+}; and Co^{2+} and Ni^{2+} induce the same change as Zn^{2+} (data not shown). It cannot be excluded at this stage that B1 binds divalent metal ions other than Zn^{2+} *in vivo*, although this

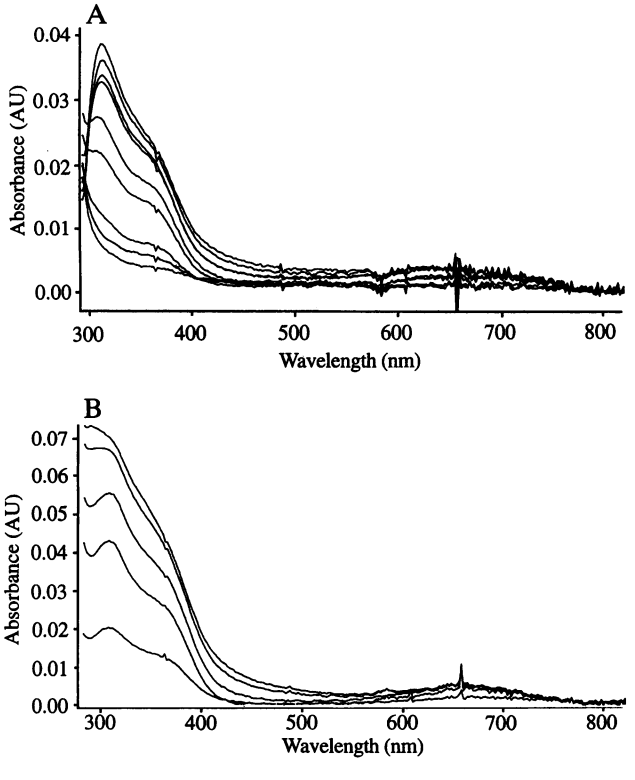

FIG. 2. Co^{2+} titration of B1 (*A*) and B2 (*B*) peptides. Spectra shown represent single experiments using 20 and 60 μM B1 and B2 peptides, respectively. For B1, Co^{2+} was added in increments from 0.2 to 25 μM. For B2, Co^{2+} was added in 5 μM increments from 1 to 20 μM.

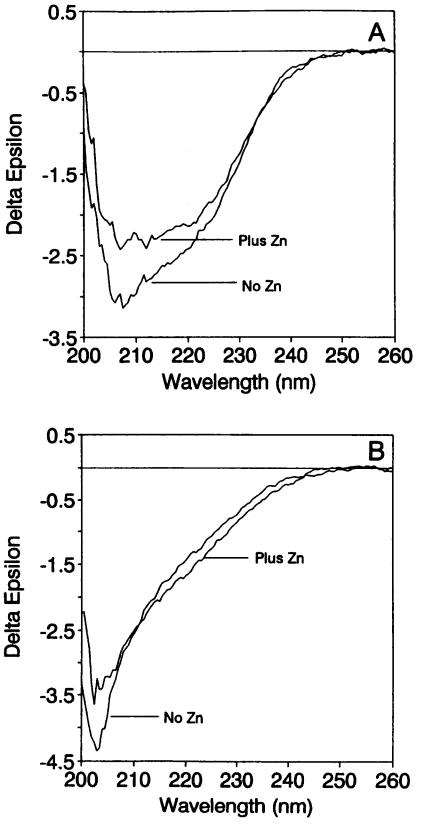

FIG. 3. CD spectra of B1 (*A*) and B2 (*B*) peptides. Peptide concentration was ≈4 μM in 5-mm cuvettes. Concentration of metal was 0.2 mM and it was added as the chloride.

analysis clearly shows that B1 can bind Zn^{2+} as effectively as Co^{2+} and/or Ni^{2+}.

Similar studies were carried out on the B2 peptide (Fig. 3*B*). B2, like the XNF7 B-box (24), appears to be largely unstructured in the absence of metal ions. The small decrease in intensity at 198 nm and the concomitant increase at 222 nm produced by the addition of Zn^{2+} indicate the formation of only a small amount of α-helix (<5%). Interestingly, the spectrum of B2 in the presence of Zn^{2+} appears to be very similar to that of the XNF7 B-box in the presence of metal (24). The only metal that produces structural changes comparable to those produced by Zn^{2+} is Co^{2+}. As in the case of XNF7 (24) and B1 (see above), the small metal-induced changes are reversed by addition of EDTA. The addition of TFE to samples of B2 in the absence of metal produces only a slight increase in helicity, indicating that this protein has little capacity for α-helix formation.

A comparison of the spectra for B1 and B2 after addition of Zn^{2+} shows significant differences (Fig. 3), suggesting that both domains have differing secondary structure compositions. Also, addition of TFE to the B1 sample causes a greater increase in helicity than for B2, further highlighting the inherent structural differences between both domains (data not shown). This indicates that like the RING finger domain, there may be some structural variability in the B-boxes. However, one would expect that the B-box metal ligands would be conserved within the B-box family as they are in the RING family.

Description of PML B-Box Mutations. The sequence homology between B-boxes and the absolute conservation of metal ligands between the different B-box family members (14) suggests that the B-box motif has a common metal ligation system. Therefore, we used the metal ligation system of the XNF7 B-box homologue as derived from the three-dimensional structure (25) to design several point mutations of PML B1 and B2. The double point mutations PML B1Cys17Cys20ΔAla, B1Cys25Cys28ΔAla, and B2Cys21Cys24ΔAla were made based on the following criteria (see Fig. 1). The B1Cys25Cys28ΔAla mutation should eliminate the Zn^{2+} binding capacity in B1 since Cys-28 was shown to be critical for metal binding and folding of the XNF7 B-box monomer structure (see Fig. 1). The other double mutations (B1Cys17Cys20ΔAla; B2Cys21Cys24ΔAla) occur on a flexible loop in the XNF7 B-box structure (see Fig. 1) and have been shown by mutational analysis in the XNF7 system not to be necessary for metal binding or folding of the monomer domain. We have proposed that these potential metal ligands are conserved in order to interact either with other proteins or with another B-box domain through a metal-mediated interaction (25).

Finally, a deletion within the PML protein was made using the restriction enzyme *Eag* I. This mutant, designated PML-Eag, had both B1 and B2 and four heptad repeats of the helical coiled-coil domain removed as shown in Fig. 1. This construct allowed us to investigate the overall contribution of both B1 and B2 in our functional assays.

Mutations in PML B1 and B2 Preclude PML Nuclear Body Formation *in Vivo*. To test the *in vivo* a functional importance of the B1, B2 metal-ligation mutants (see above), we carried out immunofluoresence studies on transiently transfected NIH 3T3 cells. It has been shown previously by us and others that transiently expressed wild-type PML in mammalian cells gives rise to a characteristic punctate nuclear staining pattern corresponding to endogenous PML nuclear bodies (5, 8–10, 16). The mutants, B1Cys17Cys20ΔAla, B1Cys25Cys28ΔAla, B2Cys21Cys24ΔAla, and wild-type PML were transiently transfected into NIH 3T3 cells and visualized using a polyclonal anti-PML antibody. The PML antibody recognizes both transfected material and the mouse PML homologue, resulting in a low level background of punctate nuclear pattern, which is easily differentiated from the intense signal due to transfected material. Our previous work has shown that peptide-purified PML antibody recognizes only human PML (16) and that the transfected PML material does not

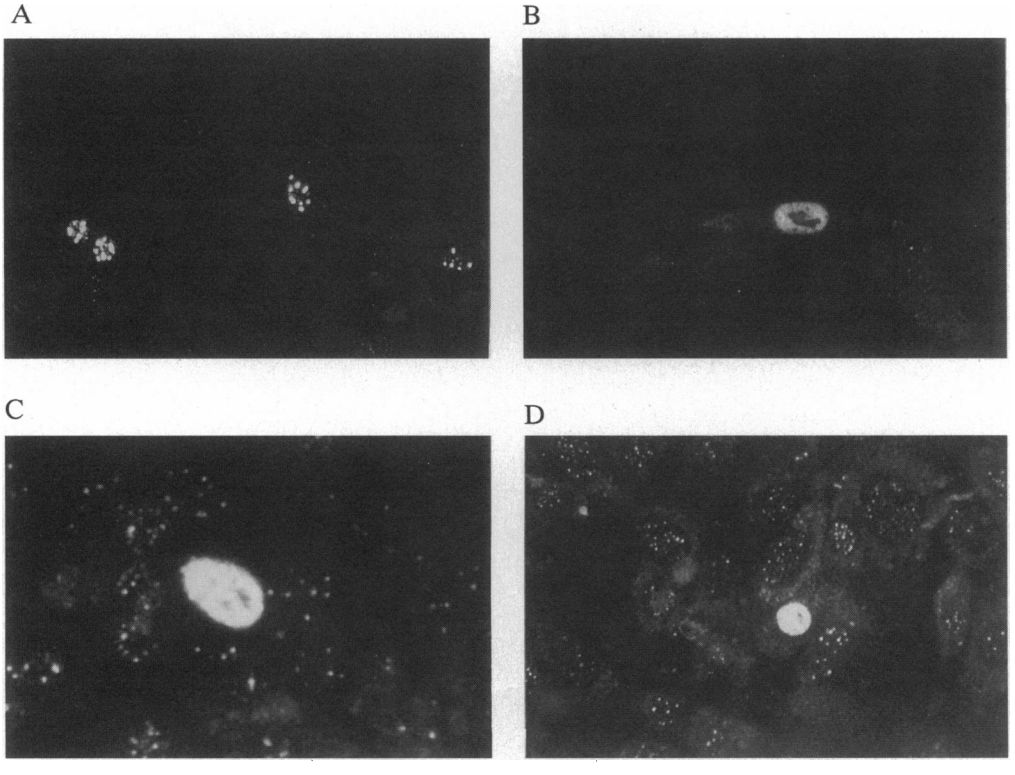

FIG. 4. Analysis of PML B1 and B2 mutants by transient transfection and indirect immunofluorescence. Fluorescence images of NIH 3T3 cells transiently transfected with wild-type (*A*); B1C17C20ΔAla (*B*); B1C25C28ΔAla (*C*), and B2C21C24ΔAla (*D*). Images were obtained from a 600 Bio-Rad confocal microscope.

appear to disrupt and/or colocalize with endogenous mouse PML nuclear bodies (data not shown). We attribute this to specific sequence differences between the mouse and human PML coiled-coil domains, both of which are essential for homodimerization *in vitro* and NB formation *in vivo* (N. Boddy and P.S.F., unpublished results). Transfected wild-type PML results in the characteristic punctate nuclear pattern (Fig. 4*A*), as observed (ref. 16 and references therein). Transfections of all three mutant PML proteins (Fig. 4 *B–D*) showed a diffuse nuclear staining pattern remaining excluded from the nucleoli. Interestingly, this is similar to our previous results for point mutations in the PML RING finger (16) but different from the phenotype observed in APL patients, which is usually microparticulate (8–10). Transfection of the PML-*Eag* mutant resulted in a low level of diffuse staining pattern throughout both the cytoplasm and nucleus with no evidence of PML nuclear body formation (data not shown).

The inability of the B1Cys25Cys28ΔAla mutant to form nuclear bodies suggests that the presence of a correctly folded B1 domain is essential for PML, nuclear body formation, as Cys-28 was shown to be critical for metal binding and folding of the XNF7 B-box monomer (25). The B1Cys17Cys20ΔAla and B2Cys21Cys24ΔAla double mutants also appear to disrupt PML nuclear body formation. Mutations of these same conserved residues in the XNF7 B-box homologue still allow folding of the B-box monomer (25). Therefore, by analogy, it is unlikely for these mutations that complete misfolding of the PML B1 and B2 domains is the cause of the dispersed PML nuclear pattern. It is possible that mutating these residues disrupts a protein–protein interface, which may be mediated by Zn^{2+} ligation as suggested for the XNF7 B-box (25). It is clear, however, that mutations of the conserved metal ligands for each PML B-box, whether involved in B-box monomer folding or in a potential metal-mediated protein–protein interface, interfere with the formation of PML nuclear bodies. It is interesting to note that we obtained similar results with the PML RING finger, where mutations of metal ligands directly involved in the folding of the RING domain also prevented PML nuclear body formation *in vivo* (16).

Mutations in B1 and B2 Do Not Affect PML's Ability to Homodimerize. The point mutations described above as well as the PML-*Eag* deletion were used in assays to ascertain whether these proteins could dimerize with wild-type PML (90-kDa isoform). Thus, we could determine whether the loss of nuclear body formation ability was linked to a loss of dimerization capacity.

The mutations/deletion were cotranslated in reticulocyte lysate (Promega) with a large isoform of PML (90 kDa), which had a C-terminal 9E10 tag. The cotranslates were then coimmunoprecipitated with the 9E10 monoclonal antibody followed by SDS/PAGE analysis. In all cases, the mutant and deletion protein were present in the precipitate, indicating that the protein's ability to form homodimers had not been impaired, examples of which are shown in Fig. 5. The ability to form dimers with wild-type PML was also monitored by the yeast two-hybrid system (38). The PML-*Eag* pAS construct interacted with the PML(pACT) construct, giving blue colonies within 1 hr (data not shown). These results indicate that the B1 and B2 domains are not required for homodimerization *in vitro*. This suggests, not unexpectedly, that the coiled-coil domain drives the dimerization *in vitro*, although the first four heptad repeats appear to be unnecessary. Perez *et al.* (11) also observed that dimerization of the PML–RARα fusion to PML *in vitro* was through regions of the helical coiled-coil region. However, our data also suggest that loss of the ability to form PML nuclear bodies is not due to loss of homodimerization capability *in vitro* but it may be attributable to some sort of homo/hetero-protein–protein interaction *in vivo*.

Implications for the Function of the Tripartite RING–B-Box–Coiled-Coil Motif. In this report, we have focused on the B-box zinc binding domains B1 and B2 from PML. This work

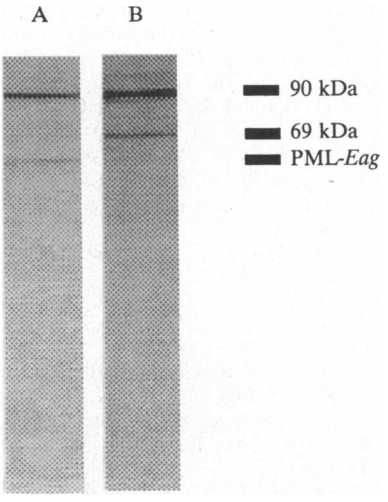

FIG. 5. Autoradiograph of coimmunoprecipitated cotranslates of a point mutation and PML-*Eag* deletion with wild-type PML plus the 9E10tag. Lanes: A, PML-*Eag*; B, B1C17C20ΔAla mutant. The 90-kDa 9E10-tagged protein is the upper band in both cases. The 69-kDa label refers to the B1C17C20ΔAla mutant.

and that reported previously (16) shows that mutations within the PML RING and B-box domains destroy the capacity of PML to associate and/or form PML nuclear bodies *in vivo*. We have also linked the structural rearrangements necessary for biological function with Zn^{2+} binding. From the homologous XNF7 B-box structure, there appear to be two classes of conserved Cys/His residues within the B-box motif: *(i)* residues directly involved in metal ligation crucial to monomer formation, and *(ii)* those residues not involved in monomer folding (25). We have shown that mutating either type of residue in the PML B1 and B2 B-boxes results in a loss of association and/or formation of nuclear bodies. Furthermore, our *in vitro* data show that the ability for PML to homodimerize is not sufficient to form nuclear bodies. Together these data suggest that the RING, B1, and B2 domains are involved in a homo/hetero-oligomerization process via protein–protein interactions central to PML nuclear body formation *in vivo*.

Interestingly, the tripartite motif is found in other proteins, TIF1 (18) and RFP (T. Cao and L. Etkin, personal communication), which are known to form large macromolecular assemblages within the nucleus, similar to PML. However, TIF1 and PML nuclear bodies appear distinct in terms of their subnuclear distribution (18), suggesting that they may function differently, which may not be surprising given TIF1's unique association with nuclear receptor activation (18). RFP nuclear bodies have not been fully characterized, although it is established that RFP like PML is tightly associated with the nuclear matrix (39, 40). PML nuclear-like bodies have also been observed in the cytoplasm for a long and short isoform of PML (41). These data suggest that the tripartite motif as found in a variety of different unrelated proteins plays a fundamental role in macromolecular targeting and/or assembly, which can occur either within or outside the nucleus, depending on other contextual cues. Several of the tripartite domains (PML, TIF1, and RFP) have oncogenic potential. This oncogenecity could well result from abnormal subcellular distribution of nuclear body components and thereby prevent normal function of the associated proteins. In APL, for example, PML nuclear bodies are disrupted (8–10). These observations linked with reports of PML growth suppressor activity (12) and linkage of PML nuclear body formation to the cell cycle (13, 40) suggest that the formation of at least PML macromolecular assemblages may involve sequestration of components involved in cell cycle control or growth regulation.

We would like to thank Nick Boddy for the PML pACT construct, PML antibody, and advice. We also thank Peter Jordan for assistance on the confocal microscope and Hans Hansen and Darryl Pappin for mass spectrometry analysis. This work is supported by the Medical Research Council (U.K.) and the Imperial Cancer Research Fund (U.K.).

1. Grignani, F., Fagioli, M., Alcalay, M., Longo, L., Pandolfi, P. P., Donti, E., Biondi, A., Lo Coco, F., Grignani, F. & Pelicci, P. G. (1994) *Blood* **83,** 10–25.
2. Goddard, A. D., Borrow, J., Freemont, P. S. & Solomon, E. (1991) *Science* **254,** 1371–1374.
3. Kakizuki, A., Miller, W. H., Umesono, K., Warrel, R. P., Jr., Frankel, S. R., Murty, V. V. V. S., Dimetrovsky, E. & Evans, R. M. (1991) *Cell* **66,** 663–674.
4. de Thé, H., Lavau, C., Marchio, A., Chomienne, C., Degos, L. & Dejean, A. (1991) *Cell* **66,** 675–684.
5. Kastner, P., Aymee, P., Lutz, Y., Rochetty-Egly, C., Gaub, M.-P., Durand, B., Lanotte, M., Berger, R. & Chambon, P. (1992) *EMBO J.* **11,** 629–642.
6. Ascoli, C. A. & Maul, G. G. (1991), *J. Cell Biol.* **112,** 785–795.
7. Zhu, Z., Cai, W. & Schaffer, P. A. (1994) *J. Virol.* **68,** 3027–3040.
8. Dyck, J. A., Maul, G. G., Miller, W. H., Chen, J. D., Kakizuka, A. & Evans, R. M. (1994) *Cell* **76,** 333–343.
9. Koken, M. H. M., Puvion-Dutilleul, F., Guillemin, M. C., Viron, A., Linares-Cruz, G., Stuurman, N., de Jong, L., Szostecki, C., Calvo, F., Chomienne, C., Degos, L., Puvion, E. and de Thé, H. (1994) *EMBO J.* **13,** 1073–1083.
10. Weis, K., Rambaus, S., Lavau, C., Jansen, J., Carvalho, T., Carmo-Fonseca, M., Lamond, A. & Dejean, A. (1994) *Cell* **76,** 345–356.
11. Perez, A., Kastner, P., Sethi, S., Lutz, Y., Reibel, C. & Chambon, P. (1993) *EMBO J.* **12,** 3171–3182.
12. Mu, Z.-M., Chin, K.-V., Liu, J.-H., Lozano, G. & Chang, K.-S. (1994) *Mol. Cell. Biol.* **14,** 6858–6867.
13. Chang, K.-S., Fan, Y.-H., Andreeff, M., Liu, J., & Mu, Z.-M. (1995) *Blood* **85,** 3646–3653.
14. Reddy, B. A., Etkin, L. D. & Freemont, P. S. (1992) *Trends Biochem. Sci.* **17,** 344–345.
15. Freemont, P. S. (1993) *Ann. N.Y. Acad. Sci.* **684,** 174–192.
16. Borden, K. L. B., Boddy, M. N., Lally, J., O'Reilly, N. J., Martin, S., Howe, K., Solomon, E. & Freemont P. S. (1995) *EMBO J.* **14,** 1532–1541.
17. Reddy, B. A. & Etkin, L. D. (1991) *Nucleic Acids Res.* **19,** 6330.
18. Le Douarin B., Zechel, C., Garnier, J.-M., Lutz, Y., Tora, L., Pierrat, B., Heery, D., Gronemeyer, H., Chambon, P. & Losson, R. (1995) *EMBO J.* **14,** 2020–2033.
19. Inoue, S., Orimo, A., Hosoi, T., Kondo, S., Toyoshima, H., Kondo, T., Ikegami, A., Ouchi, Y., Orimo, H. & Murumatsu, M. (1993) *Proc. Natl. Acad. Sci. USA* **90,** 11117–11121.
20. Campbell, I. G., Nicolai, H. M., Foulkes, W. D., Senger, G., Stamp, G. W., Allan, G., Boyer, C., Jones, K., Bast, R. C., Solomon, E., Trowsdale, J. & Black, D. M. (1994) *Hum. Mol. Genet.* **3,** 589–594.
21.. Miki, Y., Swensen, J., Shattuck-Eidens, D., Futreal, P. A., Harshman, K. *et al.* (1994) *Science* **266,** 66–71.
22. Brown, M. A.. Nicolai, H., Xu, C.-F., Griffiths, B. L., Jones, K. A., Hosking, L., Trowsdale, J., Black, D. M., McFarlane, R. & Solomon, E. (1994) *Nature (London)* **372,** 733.
23. Leonhardt, E. A., Kapp, L. N., Young, B. R. & Murnane, J. P. (1994) *Genomics* **19,** 130–136.
24. Borden, K. L. B., Martin, S. R., O'Reilly, N., Lally, J. M., Reddy, B. A., Etkin, L. D. & Freemont, P. S. (1993) *FEBS Lett.* **335,** 255–260.
25. Borden, K. L. B., Lally, J. M., Martin, S. R., O'Reilly, N. J., Etkin, L. D. & Freemont, P. S. (1995) *EMBO J.* **14,** 5947–5956.
26. Frankel, A. D., Berg, J. M. & Pabo, C. O. (1987) *Proc. Natl. Acad. Sci. USA* **84,** 4841–4845.
27. Li, X. X., Shou, W., Kloc, M., Reddy, B. A. & Etkin, L. D. (1994) *Exp. Cell Res.* **218,** 472–480.
28. Bellini, M., La Croix, J.-C. & Gall, J. G. (1993) *EMBO J.* **12,** 107–114.
29. Karas, M. & Hillenkamp, F. (1988) *Anal. Chem.* **60,** 2299–2301.
30. Mullis, K., Faloona, F., Scharf S., Saiki, R., Horn, G. & Erlich, H. (1986) *Cold Spring Harbor Symp. Quant. Biol.* **51,** 263–273.
31. Dalton, S. & Treisman, R. (1992) *Cell* **68,** 597–612.
32. Vaheri, A. & Pagano, J. S. (1965) *Virology* **27,** 434–436.
33. Sambrook, J., Fritsch, E. F. & Maniatis, T. (1989) *Molecular Cloning: A Laboratory Manual* (Cold Spring Harbor Lab. Press, Plainview, NY), 2nd Ed.
34. Rose, M. D., Winston, F. & Heiter, P. (1990) *Methods in Yeast Genetics: A Laboratory Manual* (Cold Spring Harbor Lab. Press, Plainview, NY).
35. Bertini, I. & Luchinat, C. (1984) *Advances in Inorganic Biochemistry*, eds. Eichhorn, G. L. & Marzilli, L. G. (Elsevier, New York), pp. 71–111.
36. Maret, W., Andersson, I., Dietrich, H., Schneider-Bernlohr, Einarsson, R. & Zeppezauer, M. (1979) *Eur. J. Biochem.* **98,** 501–512.
37. Berg, J. M. & Merkle, D. L. (1989) *J. Am. Chem. Soc.* **111,** 3759–3761.
38. Fields, S. & Song, O. (1989) *Nature (London)* **340,** 245–246.
39. Takahashi, M., Inaguma, Y., Hiai, H. & Hirose, F. (1988) *Mol. Cell. Biol.* **8,** 1853–1856.
40. Stuurman, N., De Graaf, A., Floore, A., Josso, A., Humbel, B., De Jong, L. & Van Driel, R. (1982) *J. Cell Sci.* **101,** 773–784.
41. Flenghi, L., Fagioli, M., Tomassoni, L., Pileri, S., Gambacorta, M., Pacini, R., Grignani, F., Casini, T., Ferrucci, P. F., Martelli, M. F., Pelicci, P.-G. & Falini, B. (1995) *Blood* **85,** 1871–1880.
42. Bellini, M., Lacroix, J.-C. & Gall, J. G. (1995) *J. Cell Biol.* **131,** 563–570.